Mauritius Research Council

A Riemann Least Squares Scheme for Inviscid Fluid Flows Problem

Final Report

April 2015

Mauritius Research Council

Address:

Level 6, Ebene Heights
34, Cybercity
Ebene

Telephone: (230) 465 1235
Fax: (230) 465 1239
E-mail: mrc@intnet.mu
Website: www.mrc.org.mu

This report is based on work supported by the Mauritius Research Council under award number MRC-RUN-1405. Any opinions, findings, recommendations and conclusions expressed herein are the author's and do not necessarily reflect those of the Council.

A Riemann Least Squares Scheme for Inviscid fluid flows problem.

Mauritius Research Council

Research Assistant: Maheshsingh Mungur

Principle Investigator: Assoc. Prof. MZ Dauhoo

Report submitted to the Mauritius Research Council

April 2015

Table of Contents

List of Figures

1 Abstract

We describe a new Riemann solver that is incorporated in the Least Squares Finite Difference Scheme which is a strong form of meshless method. We present 3 types of schemes, namely, the first order Riemann Least Squares Finite Difference Scheme (RLSFD), the conservative form of the RLSFD scheme and the second order Riemann Least Squares finite difference scheme. We then prove that the first order RLSFD is consistent with the linear advection equation and that it is conditionally stable. We also prove the existence of a weak solution for the first order RLSFD. Finally, we present our numerical results when the RLSFD is applied to the 1-D linear advection equation, 1-D Burgers equation, the Shock tube problem, the 2-D Riemann problem and to some two phase flow problems.

2 Introduction

In this report, we describe a new Riemann solver that is incorporated in the Least Squares Finite Difference Scheme which is a strong form of meshless method. In the recent years, the Godunov type methods have been succesfully applied for the inviscid compressible flows problem. Godunov type scheme is characterized by theirs robutness in calculating flow with very complicated shock structures. Godunovs method is an extension of the classical Courant-Isaacson-Rees scheme (Harten et al. 1983). A Second order extension of Godunov type method was made by Van Leer (1979) and further development was made in this field of research. The disadvantage of Godunov's method is the difficulty of solving nonlinear Riemann problem exactly which leads to a complex and time-comsuming numerical codes. To overcome these drawback, approxaimate Riemann solver have been developed. Some known approximate Riemann solver are Osher & Solomon (1982), Roe (1981) and the PPM scheme by Woodward & Colella (1984). These scheme are less costly than the exact Riemann solver. A meshless method is a method used to establish system algebraic equations for the whole problem domain without the use of a predefined mesh for the domain discretization. It uses a set of nodes scattered within the problem domain as well as sets of nodes scattered on the boundaries of the domain to represent the problem domain and its boundaries. Meshless methods are relatively new and are not mature as mesh based method including finite difference, finite element and finite volume. The advantage of meshless methods is that they provide solution accuracies for certain classes of equations that rival those of finite elements and boundary elements, without requiring the need for mesh connectivity. Meshless also requires no domain or surface discretization or numerical integration. Alternatively, a meshless method is not restricted to dimensional limitations. Meshless method doesnot capture shock as good as a Godonuv-type scheme. Therefore we incorporated a Riemann solver into the meshless scheme to capture shock and contact discontinuities more accurately.

This report is organized as follows, in section 2 we introduce the Riemann Least squares finite difference scheme for an advection equation. We present 3 types of schemes, the first order Riemann Least Squares Finite Difference Scheme (RLSFD) , the conservative form of

the RLSFD scheme and the second order Riemann Least Squares finite difference scheme. In section 3 we present the second order Least squares finite difference and extended it to a second order RLSFD scheme. In section 4, we present the proof of the weak solution of the scheme and the stability analysis of the scheme. In section 5, the RLSFD is extended in 2 dimension by applying to VOF method and a 2-D Riemann problem.

3 The Riemann Least Squares Finite Difference Scheme (RLSFD)

We consider a 1-d Linear Advection Equation given by:

$$\frac{\partial u}{\partial t} + a\frac{\partial u}{\partial x} = 0. \tag{1}$$

Using the Least squares technique, we obtain a 1^{st} order approximation of the spatial derivative of x as

$$\frac{\partial u}{\partial x} = \frac{\sum_{i=1}^{n} \Delta x_i \Delta u_i}{\sum_{i=1}^{n} \Delta x_i^2}. \tag{2}$$

Using Eq.(2), we solve the local Riemann problem within each connectivity of each node of the computational domain in the form

$$\frac{\partial u}{\partial t} + \sum_{i=1}^{n} w_i (\Delta x_i)^2 \frac{\partial u}{\partial x} = 0, \tag{3}$$

with jump $\sum_{i=1}^{n} \Delta x_i \Delta u_i$.

We assign a weight w_i to each $(\Delta x_i)^2$ on the supporting nodes in each connectivity so that $\sum_{i=1}^{n} w_i (\Delta x_i)^2$ is approximated to the speed of the exact solution. For the linear advection equation given by Eq.(1) the speed is a.

In each connectivity, we consider a jump $\sum_{i=1}^{n} \Delta x_i \Delta u_i$ which we split as a linear combination of ΔU's taken as the difference in U from two adjacent nodes within the connectivity. Thus, with a given connectivity shown in Figure 3 , we get

$$\begin{aligned}\sum_{i=1}^{n} \Delta x_i \Delta u_i = {} & \lambda_{i-3}(U_{i-2} - U_{i-3}) + \lambda_{i-2}(U_{i-1} - U_{i-2}) + \lambda_{i-1}(U_i - U_{i-1}) \\ & + \lambda_{i+1}(U_{i+1} - U_i) + \lambda_{i+2}(U_{i+2} - U_{i+1}) + \lambda_{i+3}(U_{i+3} - U_{i+2}). \end{aligned} \tag{4}$$

Following the idea of Godunov (Toro & Toro (1999)), we assume that the jump in the solution is constant between 2 nodes within the connectivity. This is illustrated in Figure 3.

Thus, for the connectivity shown in the figure,

$$\begin{aligned} [x_{m-1}, x_m] &\rightarrow \lambda_{m-1}(U_m - U_{m-1}) \quad \text{if } m \leq i, \\ [x_m, x_{m+1}] &\rightarrow \lambda_{m+1}(U_{m+1} - U_m) \quad \text{if } m \geq i. \end{aligned}$$

Eq.(4) is solved subject to the constraint $\lambda_{i-3} + \lambda_{i-2} + \lambda_{i-1} + \lambda_{i+1} + \lambda_{i+2} + \lambda_{i+3} = 1$.

By comparing the coefficient of λ in Eq.(4) we obtain the following system of equation

$$\begin{aligned} \lambda_m \Delta U_m &= \Delta x_m \Delta U_m, \\ \lambda_{i-1}\Delta U_i - \lambda_i \Delta U_i &= \Delta x_i \Delta U_i \quad i = m, \cdots, n, \\ \text{and} \quad \lambda_n \Delta U_n &= \Delta x_n \Delta U_n. \end{aligned}$$

We then minimize the following function :

$$\begin{aligned} f = (\lambda_{i-3}\Delta U_{i-3} - \Delta x_{i-3}\Delta U_{i-3})^2 + (\lambda_{i-3}\Delta U_{i-2} - \lambda_{i-2}\Delta U_{i-2} - \Delta x_{i-2}\Delta U_{i-2})^2 + \\ (\lambda_{i-2}\Delta U_{i-1} - \lambda_{i-1}\Delta U_{i-1} - \Delta x_{i-1}\Delta U_{i-1})^2 + (\lambda_{i+1}\Delta U_{i+1} - \lambda_{i+2}\Delta U_{i+1} - \Delta x_{i+1}\Delta U_{i+1})^2 + \\ (\lambda_{i+2}\Delta U_{i+2} - \lambda_{i+3}\Delta U_{i+2} - \Delta x_{i+2}\Delta U_{i+2})^2 + (\lambda_{i+3}\Delta U_{i+3} - \Delta x_{i+3}\Delta U_{i+3})^2, \quad (5) \end{aligned}$$

subject to the constraint $\lambda_{i-3} + \lambda_{i-2} + \lambda_{i-1} + \lambda_{i+1} + \lambda_{i+2} + \lambda_{i+3} = 1$.

For each connectivity we have to compute the values of $\lambda_{i-3}, \lambda_{i-2}, \lambda_{i-1}, \lambda_{i+1}, \lambda_{i+2}, \lambda_{i+3}$ and then sum all the jumps in their respective cell.

Split the jump of connectivity $\rho(x_i)$

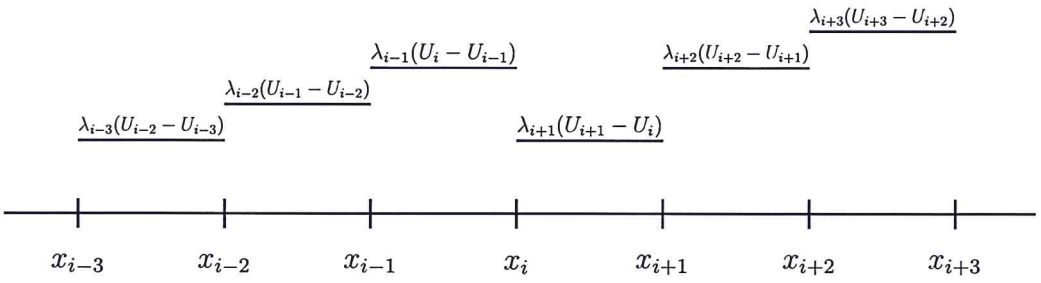

Figure 1: Split a jump in a connectivity

We denote the values of λ in the connectivity of the i^{th} node as follows:

$$\lambda_{i-3}^{(i)}, \lambda_{i-2}^{(i)}, \lambda_{i-1}^{(i)}, \lambda_{i+1}^{(i)}, \lambda_{i+2}^{(i)}, \lambda_{i+3}^{(i)}. \tag{6}$$

For a connectivity with 6 supporting nodes, there will be a maximum of 6 overlapping of jumps with the cell (x_{i-1}, x_i). The jumps in solution in cells (x_{i-1}, x_i) is denoted by D_{i-1} and it is given by

$$D_{i-1} = (\lambda_i^{(i-3)} + \lambda_i^{(i-2)} + \lambda_i^{(i-1)} + \lambda_{i-1}^{(i)} + \lambda_{i-1}^{(i+1)} + \lambda_{i-1}^{(i+2)})(U_i - U_{i-1}). \tag{7}$$

Correspondingly, D_i is the jump in $(x_i, x_i + 1)$ and it is given by

$$D_i = (\lambda_{i+1}^{(i-2)} + \lambda_{i+1}^{(i-1)} + \lambda_{i+1}^{(i)} + \lambda_i^{(i+1)} + \lambda_i^{(i+2)} + \lambda_i^{(i+3)})(U_{i+1} - U_i), \tag{8}$$

provided $a\Delta t < \Delta x_i$.

Then we advect the sum of jumps in the solution with the speed $\sum_{i=1}^{n} w_i(\Delta x_i)^2$ which is equivalent to solving a Riemann problem given by Eq.(3).

$$U_i^{n+1} = \begin{cases} U_i^n - \dfrac{a\Delta t}{\Delta x_i}(D_i) & a < 0, \\ U_i^n - \dfrac{a\Delta t}{\Delta x_i}(D_{i-1}) & a > 0. \end{cases} \tag{9}$$

Eq.(9) holds provided $a\Delta t < \Delta x_i$.

Here the $\lambda's$ of the Riemann Least squares Finite difference scheme are optimised and guarantee its meshlessness over the connectivity. We also propose a conservative form of the Riemann Least Squares Finite Difference scheme. In this scheme instead of optimising the system of Eq. (5), we force the sum of jumps in a connectivity to equal to $\alpha(U_{i+3}-U_{i-3})$. In the next subsection, we give an overview of the conservative form of the Riemann Least Squares Finite Difference scheme.

3.1 The Conservative form of the Riemann Least Squares Finite Difference scheme

We derive a conservative form of the RLSFD. Consider a 1-d linear advection equation

$$\frac{\partial u}{\partial t} + a\frac{\partial u}{\partial x} = 0. \tag{10}$$

Using the Least squares technique on the linear advection equation, we obtain an approximation of the spatial derivative of x as

$$\frac{\partial u}{\partial x} = \frac{\sum_{i=1}^{n} \Delta x_i \Delta u_i}{\sum_{i=1}^{n} \Delta x_i^2}. \tag{11}$$

Using Eq (11), we consider solving a local Riemann problem at each connectivity of the domain in the form:

$$\frac{\partial u}{\partial t} + \sum_{i=1}^{n} w_i (\Delta x_i)^2 \frac{\partial u}{\partial x} = 0, \tag{12}$$

with jump $\sum_{j=1}^{n} \Delta x_j \Delta u_j$.
For conservation the jumps must satisfies the following equation:

$$\begin{aligned}\lambda_{i-3}^{(i)}(U_{i-2} - U_{i-3}) + \lambda_{i-2}^{(i)}(U_{i-1} - U_{i-2}) + \lambda_{i-1}^{(i)}(U_i - U_{i-1}) + \lambda_{i+1}^{(i)}(U_{i+1} - U_i) \\ + \lambda_{i+2}^{(i)}(U_{i+2} - U_{i+1}) + \lambda_{i+3}^{(i)}(U_{i+3} - U_{i+2}) = \alpha(U_{i+3} - U_{i-3}),\end{aligned} \tag{13}$$

where α is a constant, $\lambda_{i\pm k}^{(i)}$, for $k = 1, 2, 3$ represent the coefficient of the difference in solution between adjacent nodes within the connectivity of the i^{th} node of the computational domain.

Solving Eq.(13) yields the following system of equation :

$$\begin{aligned}\lambda_m - \lambda_n &= 0, \\ \lambda_i - \lambda_{i+1} &= 0. \quad i = m, \cdots, n-1,\end{aligned}$$

subject to $\sum_{k=1}^{k=3} \lambda_{i\pm k} = 1$. This is equivalent to the minimization of

$$f_2 = (\lambda_{i+3}-\lambda_{i-3})^2+(\lambda_{i-3}-\lambda_{i-2})^2+(\lambda_{i-2}-\lambda_{i-1})^2+(\lambda_{i-1}-\lambda_{i+1})^2+(\lambda_{i+1}-\lambda_{i+2})^2+(\lambda_{i+2}-\lambda_{i+3})^2 \tag{14}$$

subject to $\sum_{k=1}^{k=3} \lambda_{i\pm k} = 1$.

The function f_2 is convex since it is Hessian positive semi-definite. Hence, it has a unique minimum in $\mathbb{R}^6$, when $\nabla.f = 0$. Solving the latter equation, we get $\lambda_{i-3} = \lambda_{i+3}$, $\lambda_{i-2} = \lambda_{i+3}$, $\lambda_{i-1} = \lambda_{i+3}$, $\lambda_{i+1} = \lambda_{i+3}$, $\lambda_{i+2} = \lambda_{i+3}$ and $\lambda_{i+3} = \lambda_{i+3}$, subject to the constraint $\sum_{k=-3}^{k=3} \lambda_{i+k} = 1$.

The solution is given $\lambda_{i+k} = \frac{1}{6}$, for $k = \pm 1, \pm 2, \pm 3$.

After obtaining the value of λ at each connectivity, we sum the jumps in the solution,

$$D_{i-1} = (\lambda_i^{(i-3)} + \lambda_i^{(i-2)} + \lambda_i^{(i-1)} + \lambda_{i-1}^{(i)} + \lambda_{i-1}^{(i+1)} + \lambda_{i-1}^{(i+2)})(U_i - U_{i-1}), \tag{15}$$

and

$$D_i = (\lambda_{i+1}^{(i-2)} + \lambda_{i+1}^{(i-1)} + \lambda_{i+1}^{(i)} + \lambda_i^{(i+1)} + \lambda_i^{(i+2)} + \lambda_i^{(i+3)})(U_{i+1} - U_i), \tag{16}$$

with the connectivity of each i^{th} node of the domain.

Hence, we obtain the following Riemann problem :

$$U(x) - U(x_i) = \begin{cases} D_{i-1} & \text{if } x_{i-1} < x < x_i, \\ D_i & \text{if } x_i < x < x_{i+1}. \end{cases} \tag{17}$$

The solution at the i^{th} node is then

$$U_i^{n+1} = \begin{cases} U_i^n - \dfrac{a\Delta t}{\Delta x_i}(D_i) & a < 0, \\ U_i^n - \dfrac{a\Delta t}{\Delta x_i}(D_{i-1}) & a > 0. \end{cases} \tag{18}$$

Eq.(18) holds provided $a\Delta t < \Delta x_i$.

4 Second Order Riemann Least Squares

The RLSFD scheme can be extended to a second order approach same as the second order Least Squares Finite Difference scheme using a modified difference. In this section, we introduce an overview of the Second order Least Squares Finite Difference scheme first. A

second order of LSFD scheme is derived on a linear advection equation. We start by using a taylor expansion of the supporting nodes

$$U_i = U_0 + \Delta x_i U_x + \frac{(\Delta x_i)^2}{2} U_{xx_0}, \tag{19}$$

$$\Delta U_i = \Delta x_i U_{x_0} + \mathcal{O}(\Delta x_i)^2. \tag{20}$$

Using the least squares method we obtain the spatial derivatives of x which is denoted as the first step

$$U_{x_0}^{(1)} = \frac{\sum_{i=1}^{n} \Delta x_i \Delta U_i}{\sum_{i=1}^{n} \Delta x_i^2}. \tag{21}$$

Here $U_{x_0}^{(1)}$ is first order accurate. We define a new variable

$$\Delta \tilde{U}_i = \Delta U_i - \frac{\Delta x_i}{2} \Delta U_{x_i}^{(1)}, \tag{22}$$

where $\Delta U_{x_i} = U_{x_i}^{(1)} - U_{x_0}^{(1)}$.

We define a 2 step formula for the spatial derivatives of x as

$$U_{x_0}^{(2)} = \frac{\sum_{i=1}^{n} \Delta x_i \Delta \tilde{U}_i}{\sum_{i=1}^{n} \Delta x_i^2}. \tag{23}$$

To be able to calculate the second step formula we must first calculate the first step formula given by Eq (21).

The 2 step second order formula is second order accurate.

Proof
The truncation error of $\Delta \tilde{U}_i$

$$\begin{aligned}
\Delta \tilde{U}_i &= \Delta U_i - \frac{\Delta x_i}{2} \Delta U_{x_i}^{(1)}, && (24)\\
&= \Delta x_i U_{x_0} + \frac{(\Delta x_i)^2}{2} U_{xx_0} - \frac{\Delta x_i}{2} \left(\Delta x_i U_{xx_0} + \frac{(\Delta x_i)^2}{2} U_{xxx_0} \right), && (25)\\
&= \Delta x_i U_{x_0} - \frac{(\Delta x_i)^3}{2} U_{xxx_0}. && (26)
\end{aligned}$$

The 2 step second order formula is

$$U_{x_0}^{(2)} = \frac{\sum_{i=1}^{n} \Delta x_i \Delta \tilde{U}_i}{\sum_{i=1}^{n} \Delta x_i^2}, \tag{27}$$

$$= \frac{\sum_{i=1}^{n} \left(\Delta x_i U_{x_0} - \frac{(\Delta x_i)^3}{2} U_{xxx_0} \right) \Delta x_i}{\sum_{i=1}^{n} \Delta x_i^2}, \tag{28}$$

$$= U_x - \frac{\sum_{i=1}^{n} {\Delta x_i}^4}{4 \sum_{i=1}^{n} {\Delta x_i}^4} U_{xxx_0}, \tag{29}$$

$$= U_x + \mathcal{O}(\Delta x_i^2). \tag{30}$$

We show that it is a second order accurate and we have eliminated the dissipative term U_{xx} which will reduce the dissipation of the solution.

4.1 Second order Riemann LFSD scheme for a linear advection

We consider a linear advection equation

$$\frac{\partial u}{\partial t} + a \frac{\partial u}{\partial x} = 0. \tag{31}$$

Solving Eq (31) by using a 2 step second order formula we obtain the spatial derivatives as x as

$$\frac{\partial u}{\partial x} = \frac{\sum_{i=1}^{n} \Delta x_i \Delta \tilde{U}_i}{\sum_{i=1}^{n} \Delta x_i^2}, \tag{32}$$

where $\Delta \tilde{U}_i = \Delta U_i - \frac{\Delta x_i}{2} \Delta U_{x_i}^{(1)}$.

Next, in each connectivity we solve a riemann problem given by Eq (33).

$$\frac{\partial u}{\partial t} + \sum_{i=1}^{n} w_i (\Delta x_i)^2 \frac{\partial u}{\partial x} = 0 \tag{33}$$

with jump $\sum_{i=1}^{n} \Delta x_i \Delta \tilde{U}_i$.

Next, for each connectivity we split the jump into jumps in the solution in each cell as

$$\sum_{i=1}^{n} \Delta x_i \Delta \tilde{U}_i = \lambda_{i-3}(\Delta \tilde{U}_{i-2} - \Delta \tilde{U}_{i-3}) + \lambda_{i-2}(\Delta \tilde{U}_{i-1} - \Delta \tilde{U}_{i-2}) + \lambda_{i-1}(-\Delta \tilde{U}_{i-1}) + \lambda_{i+1}(\Delta \tilde{U}_{i+1}) + \lambda_{i+2}(\Delta \tilde{U}_{i+2} - \Delta \tilde{U}_{i+1}) + \lambda_{i+3}(\Delta \tilde{U}_{i+3} - \Delta \tilde{U}_{i+2}), \quad (34)$$

where $\Delta \tilde{U}_i = \Delta U_i - \frac{\Delta x_i}{2} \Delta U_{x_i}^{(1)}$ and $\lambda_{i-3} + \lambda_{i-2} + \lambda_{i-1} + \lambda_{i+1} + \lambda_{i+2} + \lambda_{i+3} = 1$. This is a minimizing process subject to a constraint. For conservation of jumps we obtain the value of $\lambda_{i-3} = \lambda_{i-2} = \lambda_{i-1} = \lambda_{i+1} = \lambda_{i+2} = \lambda_{i+3} = \frac{1}{6}$ for 6 supporting nodes.

Having found the values of λ for each connectivity we sum the jump as a jumpof the solution w.r.t to $\tilde{U}_i$ to be constant in their respective cells. We denote D_{i-1} to be the sum of jump of the solution in cell (x_{i-1}, x_i) and D_i in the cell (x_i, x_{i+1}).

$$D_{i-1} = (\lambda_i^{(i-3)} + \lambda_i^{(i-2)} + \lambda_i^{(i-1)} + \lambda_{i-1}^{(i)} + \lambda_{i-1}^{(i+1)} + \lambda_{i-1}^{(i+2)})(\tilde{U}_i - \tilde{U}_{i-1}), \quad (35)$$

and

$$D_i = (\lambda_{i+1}^{(i-2)} + \lambda_{i+1}^{(i-1)} + \lambda_{i+1}^{(i)} + \lambda_i^{(i+1)} + \lambda_i^{(i+2)} + \lambda_i^{(i+3)})(\tilde{U}_{i+1} - \tilde{U}_i), \quad (36)$$

provided $a\Delta t < \Delta x_i$.

The scheme becomes

$$U_i^{n+1} = U_i^n - \frac{a\Delta t}{\Delta x_i}(D_{i-1}) \quad \text{if } a < 0, \quad (37)$$

$$U_i^{n+1} = U_i^n - \frac{a\Delta t}{\Delta x_i}(D_i) \quad \text{if } a > 0. \quad (38)$$

Eq (37) and (38) hold provided $a\Delta t < \Delta x_i$.

For the second order approach of the RLSFD scheme, the truncation error can be further minimized by optimising the value of $\lambda_{j,i}$ for each connectivity. We analyze the solution set of $\lambda's$ for the optimised problem. Without any loss of generality , we consider a connectivity of six supporting nodes . For the Riemann Least Squares Finite difference scheme, at each reference node j we split the jump which is given by

$$\left(\sum_{i=j-3}^{i=j+3} \Delta x_i \Delta \tilde{U}_i \right)_j, \quad (39)$$

where $\Delta \tilde{U}_i = \Delta U_i - \frac{\Delta x_i}{2} \Delta U_{x_i}^{(1)}$, throughout the connectivity in each cell of the connectivity. For example, for a reference node j we obtain the first order derivatives as an approximation

of

$$\left(\sum_{i=j-3}^{j-1}\lambda_{j,i}+\sum_{i=j}^{j+2}\lambda_{j-1,i}\right)U_{x_j}+\left[\sum_{i=j-3}^{j-1}\lambda_{j,i}(x_i-x_j)+\sum_{i=j+1}^{j+2}\lambda_{j-1,i}(x_i-x_j)\right]U_{xx_j}+$$
$$(\sum_{i=j-3}^{j-2}\lambda_{j,i}(2x_i-x_{j-1}-x_j)(x_i-x_j)-\lambda_{j-1,j}(x_{j-1}-x_j)^2+$$
$$\sum_{i=j+1}^{j+2}\lambda_{j-1,i}(x_{j-1}+x_j-2x_i)(x_{j-1}-x_i))U_{xxx_j}. \quad (40)$$

We can choose the value of λ in each connectivity throughout the whole computational mesh so that it become second order . To achieve this we have to use optimization. This is equivalent to minimizing a set of objective functions subject to a set of constraint . This is given by a multi-objective function as

$$\min\{F_1(X),\cdots,F_j(X),\cdots,F_n(X)\}, \quad (41)$$

where $F_j(X)=\sum_{\substack{i=j-3\\ i\neq j}}^{j+3}\lambda_{i,j}-1$, and the set of constraint S is given by

1.
$$\sum_{i=j-3}^{j-1}\lambda_{j,i}+\sum_{i=j}^{j+2}\lambda_{j-1,i}=1, \quad \text{for } j=1,\cdots,n \quad (42)$$

2.
$$\sum_{i=j-3}^{j-1}\lambda_{j,i}(x_i-x_j)+\sum_{i=j+1}^{j+2}\lambda_{j-1,i}(x_i-x_j)=0 \quad \text{for } j=1,\cdots,n \quad (43)$$

3.
$$\sum_{i=j-3}^{j-2}\lambda_{j,i}(2x_i-x_{j-1}-x_j)(x_i-x_j)-\lambda_{j-1,j}(x_{j-1}-x_j)^2+\sum_{i=j+1}^{j+2}\lambda_{j-1,i}(x_{j-1}+x_j-2x_i)(x_{j-1}-x_i)$$
$$-\gamma_{j,1}(x_j-x_{j-1})^2-\gamma_{j,2}(x_{j+1}-x_j)^2=0, \quad \text{for } j=1,\cdots,n. \quad (44)$$

where n is the number of nodes in the computational domain.

By using the $\epsilon-$constraints method , we choose one objective out of n to be minimized and the remaining objectives are constrained to be less than or equal to given target values. By using the following theorem we can show that there exist a weak Pareto optimum.
If an objective j and a vector $\epsilon=(\epsilon_1,\cdots,\epsilon_{j-1},\epsilon_{j+1},\cdots,\epsilon_n)\in\mathbb{R}^{n-1}$ exist, such that x^* is an optimal solution to the following problem :

$$\min F_j(x), \quad (45)$$

subject to the constraint

$$F_j(x) \leq \epsilon_i \; \forall i \; \in \{1, \cdots, n\} \backslash \{j\} \tag{46}$$
$$x \in S,$$

then x^* is a weak Pareto optimum.

The objective function $F_j(X) = \sum_{\substack{i=j-3 \\ i \neq j}}^{j+3} \lambda_{i,j} - 1$ is linear and therefore convex and the constraint $F_j(x) \leq \epsilon_i \; \forall i \; \in \{1, \cdots, n\} \backslash \{j\}$ is also convex. The set of constraints S is convex since each constraint is linear.

5 Weak solution of the RLSFD

We show that the Riemann LSFD converge to the weak solution of the conservation law:

$$\frac{\partial u}{\partial t} + \frac{\partial f(u)}{\partial x} = 0 \tag{47}$$

Theorem: Lax and Wendroff (LeVeque (2002))
Consider a sequences of grids indexed by $j = 1, 2, ...$, with mesh parameter $\Delta t^{(j)}, \Delta x^{(j)} \to 0$ as $j \to \infty$. Let $U^{(j)}(x, t)$ denote the numerical approximation computed with a conservative method on the j^{th} grid. Suppose that $U^{(j)}$ converges to a function u as $j \to \infty$, in the sense made precise below. Then $u(x, t)$ is a weak solution of the conservation law.

We assume the following conditions:

1. Over every bounded set $\Omega = [a, b] \times [0, T]$ in $x - t$ space, $||U^{(j)} - u||_{1,\Omega} \to 0$ as $j \to \infty$.
2. For each T there is an R > 0 such that $TV(U^{(j)}(., t)) < R$ for all $0 \leq t \leq T, j = 1, 2, ...,$ where TV denotes the total variation function.

In order to use the Lax and Wendroff theorem we must prove that the Riemann LSFD scheme satisfies the 2 assumptions given above.
First we prove that our scheme is consistent in 1-norm to satisfy assumption 1.

$$||U_i^{n+1} - u(x_i^n, t_{n+1})|| = ||U_i^{n+1} - u(x_i, t_{n+1})|| \tag{48}$$
$$= ||U_i^n - \frac{a\Delta t}{\Delta x_i} \tau_i (U_i^n - U_{i-1}^n) - u(x_i, t_{n+1})||, \tag{49}$$

where $\tau_i = \lambda_i^{(i-3)} + \lambda_i^{(i-2)} + \lambda_i^{(i-1)} + \lambda_{i-1}^{(i)} + \lambda_{i-1}^{(i+1)} + \lambda_{i-1}^{(i+2)}$.

$$= ||u(x_i,t_n) - \frac{a\Delta t}{\Delta x_i}\tau_i[u(x_i,t_n) - u(x_{i-1},t_n)] - u(x_i,t_{n+1})|| \quad (50)$$

$$= ||u(x_i,t_n) - \frac{a\Delta t}{\Delta x_i}\tau_i(u(x_i,t_n) - u(x_{i-1},t_n)) - [u(x_i,t_n) + \Delta t u_x(x_i,t_n)]||$$

$$= ||u(x_i,t_n) - \frac{a\Delta t}{\Delta x_i}\tau_i[u(x_i,t_n) - u(x_i,t_n) + \Delta x u_x(x_i,t_n)] - [u(x_i,t_n) + \Delta t u_x(x_i,t_n)]||$$

$$= ||\Delta t u_x(x_i,t_n) + \Delta t\tau_i u_x(x_i,t_n)|| \quad (51)$$

as $\Delta t \to 0 \quad ||\Delta t u_x(x_i,t_n) + a\Delta t\tau_i u_x(x_i,t_n)|| \to 0.$

We show that $||U^{(j)} - u||_{1,\Omega} \to 0$.

Next we show that the scheme is TVB that is, it satisfies assumption 2 .

$$TV(U_i^{n+1}) = \sum_{i=-\infty}^{\infty} |U_i^{n+1} - U_{i-1}^{n+1}| \quad (52)$$

$$= \sum_{i=-\infty}^{\infty} |U_i^n - \frac{a\Delta t}{\Delta x}\tau(U_i^n - U_{i-1}^n) - (U_{i-1}^n - \frac{a\Delta t}{\Delta x}\tau(U_{i-1}^n - U_{i-2}^n))|$$

$$= \sum_{i=-\infty}^{\infty} (1 - \frac{a\Delta t}{\Delta x}\tau)|U_i^n - U_{i-1}^n| + \frac{a\Delta t}{\Delta x}\tau|U_{i-1}^n - U_{i-2}^n|$$

$$\leq (1 - \frac{a\Delta t}{\Delta x}\tau)\sum_{i=-\infty}^{\infty} |U_i^n - U_{i-1}^n| + \frac{a\Delta t}{\Delta x}\tau\sum_{i=-\infty}^{\infty} |U_{i-1}^n - U_{i-2}^n|$$

$$= TV(U^n) - \frac{a\Delta t}{\Delta x}\tau TV(U^n) + \frac{a\Delta t}{\Delta x}TV(U^n), \quad (53)$$

since $0 \leq \frac{a\Delta t}{\Delta x} \leq 1$ and $\tau > 0$ then

$$TV(U^{n+1}) \leq TV(U^n)$$

,

$$TV(U^n) \leq TV(U^0)$$

. Therefore the scheme is TVB and hence using the Theorem of Lax and Wendroff, $u(x,t)$ obtained by RLSFD is a weak solution of Eq (47).

The Riemann LSFD is a Reconstruction-Evolution-Average algorithm. The Reconstruction phase consist of the splitting of the jump $\sum \Delta x_i \Delta U_i$ over the connectivity. Whilst the Evolution phase is the evaluation of the flux at the interface of each interval. Next we show that the weak solution $u(x,t)$ obtained as the limits of $U^{(j)}$ satisfies the entropy condition

which can be written as follows:

$$\frac{\partial \eta(q)}{\partial t} + \frac{\partial \psi(q)}{\partial x} \leq 0, \tag{54}$$

where $\eta(q)$ is a convex scalar entropy function and $\psi(q)$ is the entropy flux.

In weak sense, that is, $\forall \phi \in C_0^1 \, \forall x, t \in \mathbb{R}$, we have

$$\int_0^\infty \int_{-\infty}^\infty [\phi_t(x,t)\eta(q(x,t)) + \phi_x(x,t)\psi(q(x,t)]dx\,dt + \int_{-\infty}^\infty \phi(x,0)\eta(q(x,0))dx \geq 0. \tag{55}$$

It is sufficient to show that a discrete entropy inequality holds

$$\eta(Q_i^{n+1}) \leq \eta(Q_i^n) - \frac{\Delta t}{\Delta x}(\Psi^n_{i+\frac{1}{2}} - \Psi^n_{i-\frac{1}{2}}). \tag{56}$$

Integrate Eq.(54), we obtain

$$\int_{x_{i-\frac{1}{2}}}^{x_{i+\frac{1}{2}}} \eta(q(x,t_{n+1}))dx \leq \int_{x_{i-\frac{1}{2}}}^{x_{i+\frac{1}{2}}} \eta(q(x,t_n))dx + \int_{t_n}^{t_{n+1}} \psi(q(x_{i-\frac{1}{2}}))dt - \int_{t_n}^{t_{n+1}} \psi(q(x_{i+\frac{1}{2}}))dt, \tag{57}$$

since q is constant on the right hand side of Eq.(57) dividing by Δx yields

$$\frac{1}{\Delta x}\int_{x_{i-\frac{1}{2}}}^{x_{i+\frac{1}{2}}} \eta(q(x,t_{n+1}))dx \leq \eta(Q_i^n) - \frac{\Delta t}{\Delta x}(\Psi^n_{i+\frac{1}{2}} - \Psi^n_{i-\frac{1}{2}}), \tag{58}$$

since the entropy function η is convex we can use Jensen's inequality

$$\eta\left(\frac{1}{\Delta x}\int_{x_{i-\frac{1}{2}}}^{x_{i+\frac{1}{2}}} q(x,t_{n+1})dx\right) \leq \frac{1}{\Delta x}\int_{x_{i-\frac{1}{2}}}^{x_{i+\frac{1}{2}}} \eta(q(x,t_{n+1}))dx. \tag{59}$$

This yields

$$\eta(Q_i^{n+1}) \leq \eta(Q_i^n) - \frac{\Delta t}{\Delta x}(\Psi^n_{i+\frac{1}{2}} - \Psi^n_{i-\frac{1}{2}}). \tag{60}$$

This satisfies the discrete entropy inequality.

We also proved that the RLSFD scheme with jumps is consistent with the linear advection equation. We show that the scheme

$$\frac{\partial u}{\partial t} + \sum_{i=1}^{n} w_i(\Delta x_i)^2 \frac{\partial u}{\partial x} = \sum \Delta x_i \Delta u_i, \tag{61}$$

is consistent with

$$\frac{\partial u}{\partial t} + a\frac{\partial u}{\partial x} = 0. \tag{62}$$

Proof
Taking $\lim_{\Delta x_i \to 0}$ of Eq (61) we obtain

$$\frac{\partial u}{\partial t} + \lim_{\Delta x_i \to 0} \sum_{i=1}^{n} w_i (\Delta x_i)^2 \frac{\partial u}{\partial x} = \lim_{\Delta x_i \to 0} \sum \Delta x_i \Delta u_i \tag{63}$$

$$\frac{\partial u}{\partial t} + \frac{\partial u}{\partial x} \lim_{\Delta x_i \to 0} \sum_{i=1}^{n} w_i (\Delta x_i)^2 = \lim_{\Delta x_i \to 0} \sum \Delta x_i \Delta u_i \tag{64}$$

We choose w_i such that $\sum_{i=1}^{n} w_i (\Delta x_i)^2 \to a$

$$\begin{aligned} \frac{\partial u}{\partial t} + a\frac{\partial u}{\partial x} &= \lim_{\Delta x_i \to 0} \sum \Delta x_i (u_i - u_0) && (65) \\ &= \lim_{\Delta x_i \to 0} \sum \Delta x_i (u_0 + \Delta x_i \frac{\partial u}{\partial x} + \frac{(\Delta x_i)^2}{2} \frac{\partial^2 u}{\partial x^2} - u_0) && (66) \\ &= \lim_{\Delta x_i \to 0} \sum \Delta (x_i)^2 \frac{\partial u}{\partial x} + \lim_{\Delta x_i \to 0} \sum \frac{\Delta (x_i)^3}{2} \frac{\partial^2 u}{\partial x^2}. && (67) \end{aligned}$$

We assume that $\frac{\partial u}{\partial x}$ and $\frac{\partial^2 u}{\partial x^2}$ is bounded then

$$\begin{aligned} \frac{\partial u}{\partial t} + a\frac{\partial u}{\partial x} &= \frac{\partial u}{\partial x} \lim_{\Delta x_i \to 0} \sum \Delta (x_i)^2 + \frac{\partial^2 u}{\partial x^2} \lim_{\Delta x_i \to 0} \sum \frac{\Delta (x_i)^3}{2} && (68) \\ &= 0. && (69) \end{aligned}$$

The RLSFD scheme is said to be stable iff it satisfies the CFL condition. The scheme for $a > 0$ becomes

$$U_i^{n+1} = U_i^n - \frac{a\Delta}{\Delta x_i}(D_{i-1}), \tag{70}$$

where $D_{i-1} = (\lambda_i^{(i-3)} + \lambda_i^{(i-2)} + \lambda_i^{(i-1)} + \lambda_{i-1}^{(i)} + \lambda_{i-1}^{(i+1)} + \lambda_{i-1}^{(i+2)})(U_i - U_{i-1})$.

It becomes

$$\begin{aligned} U_i^{n+1} &= U_i^n - \alpha(U_i^n - U_{i-1}^n) && (71) \\ &= (1-\alpha)U_i^n + \alpha U_{i-1}^n, && (72) \end{aligned}$$

where $\alpha = \frac{a\Delta t}{\Delta x_i}(\lambda_i^{(i-3)} + \lambda_i^{(i-2)} + \lambda_i^{(i-1)} + \lambda_{i-1}^{(i)} + \lambda_{i-1}^{(i+1)} + \lambda_{i-1}^{(i+2)})$.

For stability we require

$$|1 - \alpha| + |\alpha| \leq 1. \tag{73}$$

Proof

$$\begin{aligned}
\sum_{i=-\infty}^{\infty} |U_i^{n+1}|^2 &= \sum_{i=-\infty}^{\infty} |(1-\alpha)U_i^n + \alpha U_{i-1}^n|^2 \\
&\leq \sum_{i=-\infty}^{\infty} \left(|1-\alpha|^2|U_i^n|^2 + 2|1-\alpha||\alpha||U_i^n||U_{i-1}^n| + |\alpha|^2|U_{i+1}^n|^2\right) \\
&\leq \sum_{i=-\infty}^{\infty} |1-\alpha|^2|U_i^n|^2 + |1-\alpha||\alpha|(|U_i^n|^2 + |U_{i-1}^n|^2) + |\alpha|^2|U_{i-1}^n|^2 \\
&= \sum_{i=-\infty}^{\infty} |1-\alpha|^2|U_i^n|^2 + |1-\alpha||\alpha||U_i^n|^2 + \sum_{i=-\infty}^{\infty} |1-\alpha||\alpha||U_{i-1}^n|^2 + |\alpha|^2|U_{i-1}^n|^2 \\
&= \sum_{i=-\infty}^{\infty} |1-\alpha|^2|U_i^n|^2 + |1-\alpha||\alpha||U_i^n|^2 + \sum_{i=-\infty}^{\infty} |1-\alpha||\alpha||U_i^n|^2 + |\alpha|^2|U_i^n|^2 \\
&= \sum_{i=-\infty}^{\infty} (|1-\alpha| + |\alpha|)^2|U_i^n|^2 \\
&= (|1-\alpha| + |\alpha|)^2 \sum_{i=-\infty}^{\infty} |U_i^n|^2.
\end{aligned}$$

$$\therefore \sum_{i=-\infty}^{\infty} |U_i^{n+1}|^2 \leq (|1-\alpha| + |\alpha|)^2 \sum_{i=-\infty}^{\infty} |U_i^n|^2,$$

and since this applies to all n, we get

$$\sum_{i=-\infty}^{\infty} |U_i^n|^2 \leq (|1-\alpha| + |\alpha|)^{2n} \sum_{i=-\infty}^{\infty} |U_i^0|^2, \tag{74}$$

stable provided $|1-\alpha| + |\alpha| \leq 1$.

6 Numerical Experiment

6.1 Linear Advection Equation

In the section, we test the Riemann Least Squares Finite Difference scheme (RLFSD) on various test case problems. First, we compare the Godunov scheme with the RLSFD for a linear advection equation. We conduct our experiment on a 1-d linear advection equation:

$$\frac{\partial u}{\partial t} + 0.2\frac{\partial u}{\partial x} = 0, \quad x \in [0,1], \tag{75}$$

with initial condition

$$u(x,0) = \begin{cases} 1 & 0.2 < x < 0.4, \\ 0 & \text{otherwise.} \end{cases} \tag{76}$$

We choose $\Delta t = 0.01$ and a non-uniform gird of 50 point.

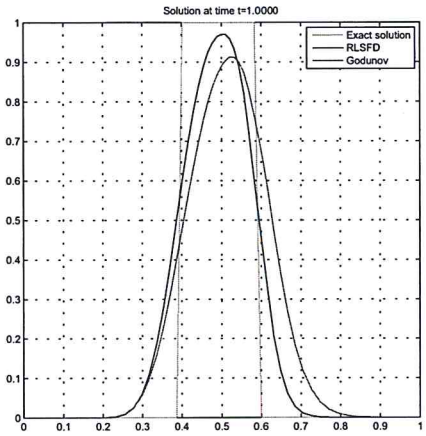

Figure 2: The RLSFD and Godunov scheme for speed 0.2

Fig.(2) shows the exact solution and the numerical solution advected at a speed of $a = 0.2$, till $t = 1s$. We see that both schemes are dissipative. However, the Riemann LSFD is less dissipative than the Godunov scheme.

Fig.(3) shows the result for $a = 0.5$, $\Delta t = 0.01$, total advection from $t = 1s$.

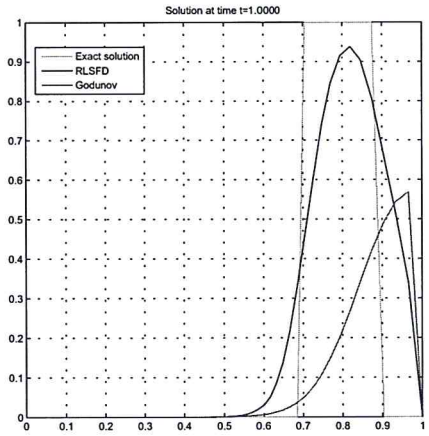

Figure 3: RLSFD and the Godunov scheme with speed 0.5

Fig. (3) shows that the Godunov scheme is highly damped whereas the RLSFD has dissipated by about 10%.

Figs. (4) and (5) show the numerical solution on a refined mesh of 100 nodes.

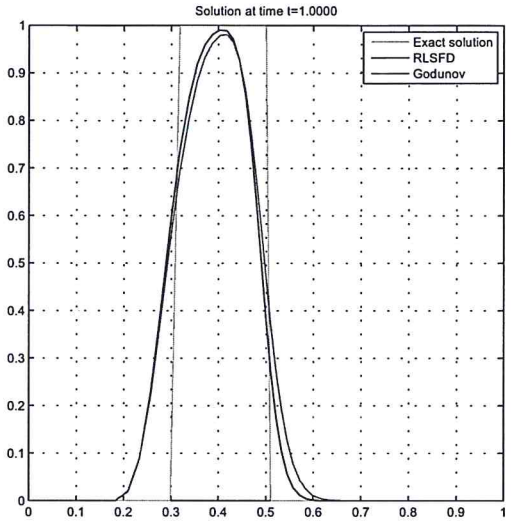

Figure 4: Rieman LSFD with 50 nodes

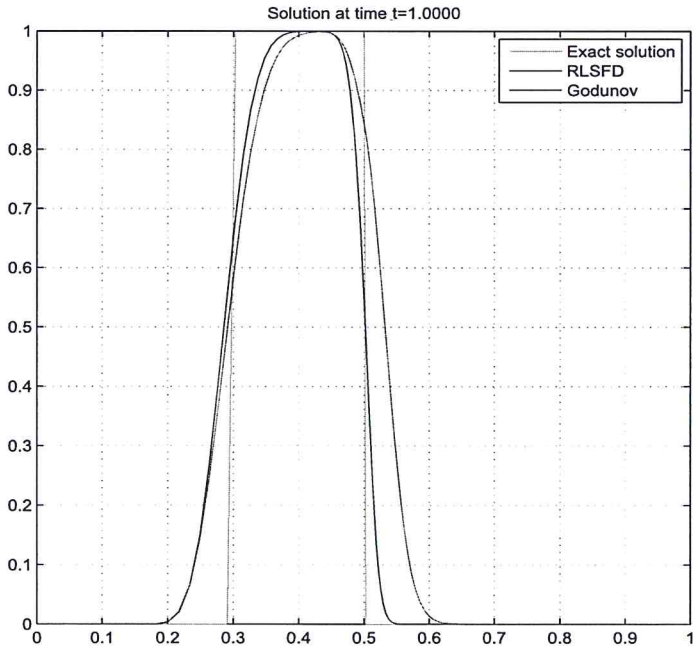

Figure 5: Riemann LSFD with 100 nodes

In this example we consider a Burgers equation to test a scheme that captures shock accurately. We perform numerical experiment on the burgers equation.

$$\frac{\partial u}{\partial t} + \frac{1}{2}u\frac{\partial u}{\partial x} = 0. \tag{77}$$

$$u(x,0) = \begin{cases} 1 & 0 < x < 0.2, \\ 0 & \text{otherwise} \end{cases} \tag{78}$$

We choose $\Delta t = 0.01$ and a non -uniform grid of 50 nodes. This is at time $t = 1$.

From Fig.(6) we observe that Godunov scheme which is the red line has overestimate the location of shock. The exact solution is show in green. The Riemann LSFD, shown in blue, locates the shock speed of the burgers equation, exactly(Toro & Toro 1999).

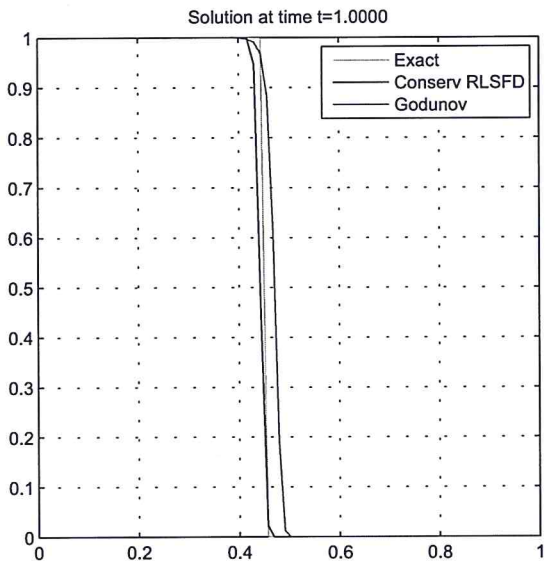

Figure 6: Riemann LSFD and godunov scheme on burgers equation

6.2 Sod shock tube problem

The RLSFD scheme is said to be a shock capturing method that capture shock and rarefaction accurately . We test the RLSFD scheme for the Sod shock-tube problem. A one

dimensional equation of the Euler equation is written in conservative form as follows:

$$\frac{\partial \rho}{\partial t} + \frac{\partial}{\partial x}(\rho u) = 0, \tag{79}$$

$$\frac{\partial}{\partial t}(\rho u) + \frac{\partial}{\partial x}(\rho u^2 + p) = 0, \tag{80}$$

$$\frac{\partial E}{\partial t} + \frac{\partial}{\partial x}(u(E+p)) = 0. \tag{81}$$

This can be written in matrix form as a non linear hyperbolic conservation laws

$$\frac{\partial U}{\partial t} + \frac{\partial}{\partial x}(F(U)) = 0, \tag{82}$$

where $U = \begin{pmatrix} \rho \\ \rho u \\ E \end{pmatrix}$ and $F(U) = \begin{pmatrix} \rho u \\ \rho u^2 + p \\ u(E+p) \end{pmatrix}$.

In the terminology of gas dynamics, the presence of discontinuity in the initial condition corresponds to a system having a shock wave, rarefaction wave and a contact discontinuity wave. With different configurations of the initial condition, not all waves may be present but in a sod-shock tube problem each of the wave is present (Toro & Toro 1999). The initial condition of a Sod shock-tube problem in the domain $0 \leq x \leq 1$ is given as

$$\rho(x,0) = \begin{cases} 1 & x \leq 0.5 \\ 0.125 & x > 0.5 \end{cases} \quad p(x,0) = \begin{cases} 1 & x \leq 0.5 \\ 0.1 & x > 0.5 \end{cases} \quad \text{and } u(x,0) = 0.$$

We perform the numerical experiment of the RLSFD scheme for the sod shock tube problem on a 50 non-uniform nodes. We use an approximate Riemann solver known as PVRS for finding the intermediate state in each primitive variable.

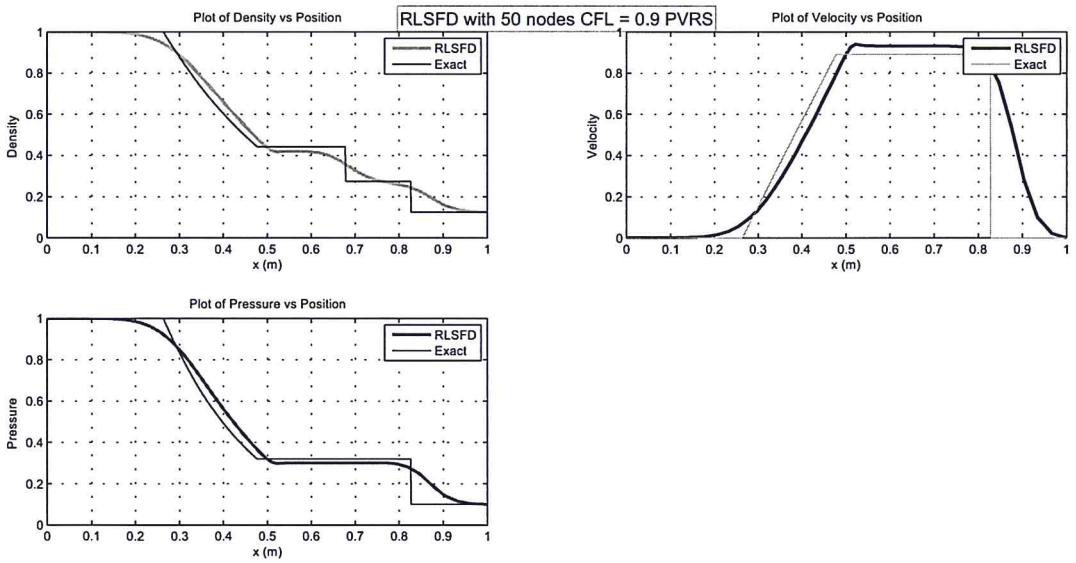

Figure 7: The RLSFD scheme at $t = 0.2$

Next, we use an exact Riemann solver for finding the intermediate state of the primitive variable for 50 non-uniform nodes and observed that the CFL has to be below 0.5. Thus more computational time is needed when using the exact Riemann solver for sod shock-tube problem.

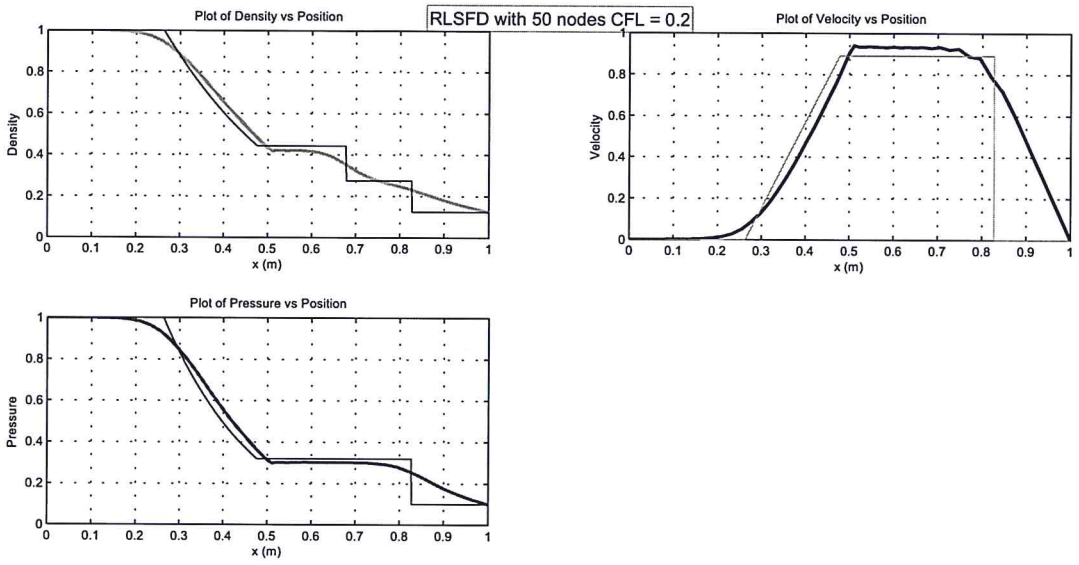

Figure 8: The RLSFD scheme with Exact Riemann solver at $t = 0.2$

In the next two experiments, we increase the computational nodes from 50 to 100 nodes. We compared the the PVRS solver with the exact Riemann solver in the 2 figures below.

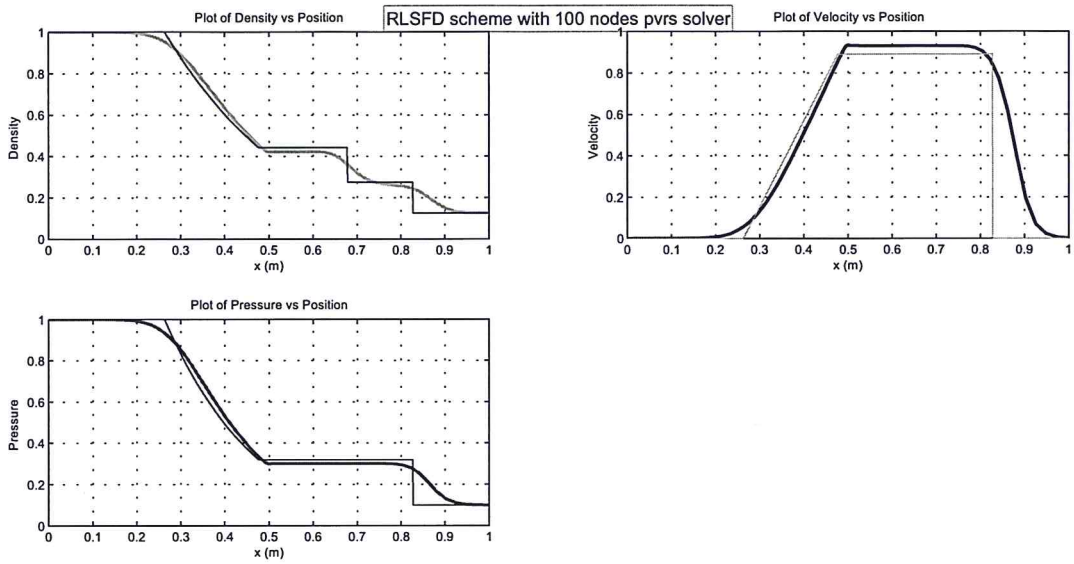

Figure 9: The RLSFD scheme with Exact Riemann solver at $t = 0.2$

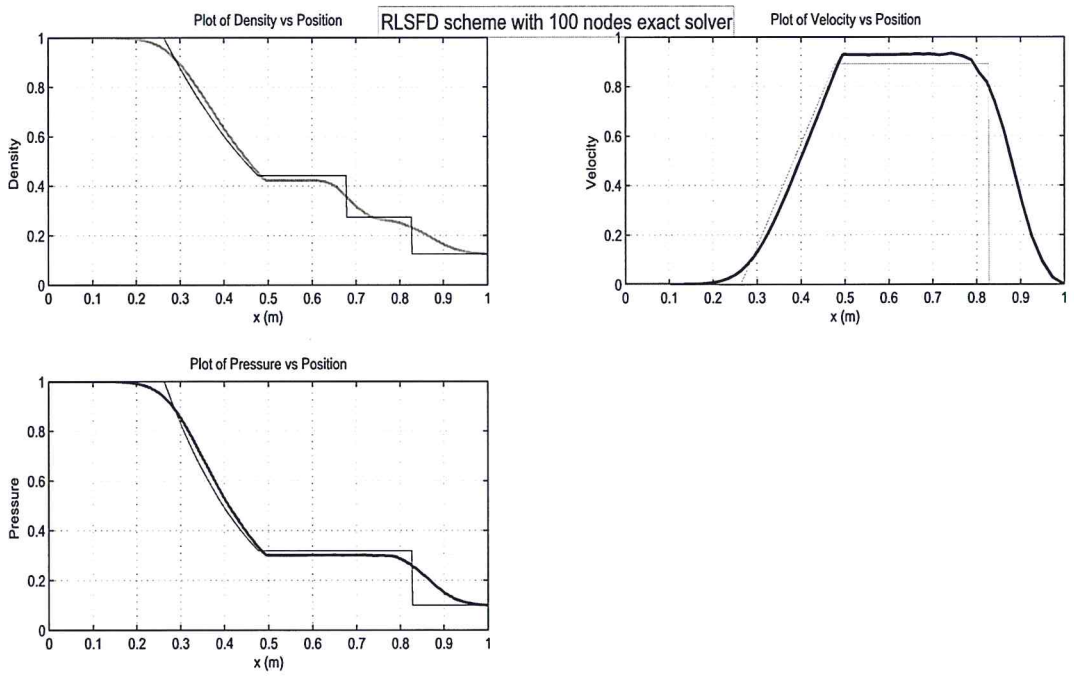

Figure 10: The RLSFD scheme with Exact Riemann solver at $t = 0.2$

This method is extended to a higher order method by choosing the jumps to be in the second order least squares derivative given by $\sum_{i=1}^{n} \Delta x_i \Delta F(\tilde{U}_i)$, where $\Delta\tilde{U}_i = \Delta U_i - \Delta x_i \Delta U_{x_i}^{(1)}$, where $U_{x_i}^{(1)}$ is the first order least squares derivative.

We perform an experiment on a second order RLSFD scheme using a PVRS solver with 100 nodes

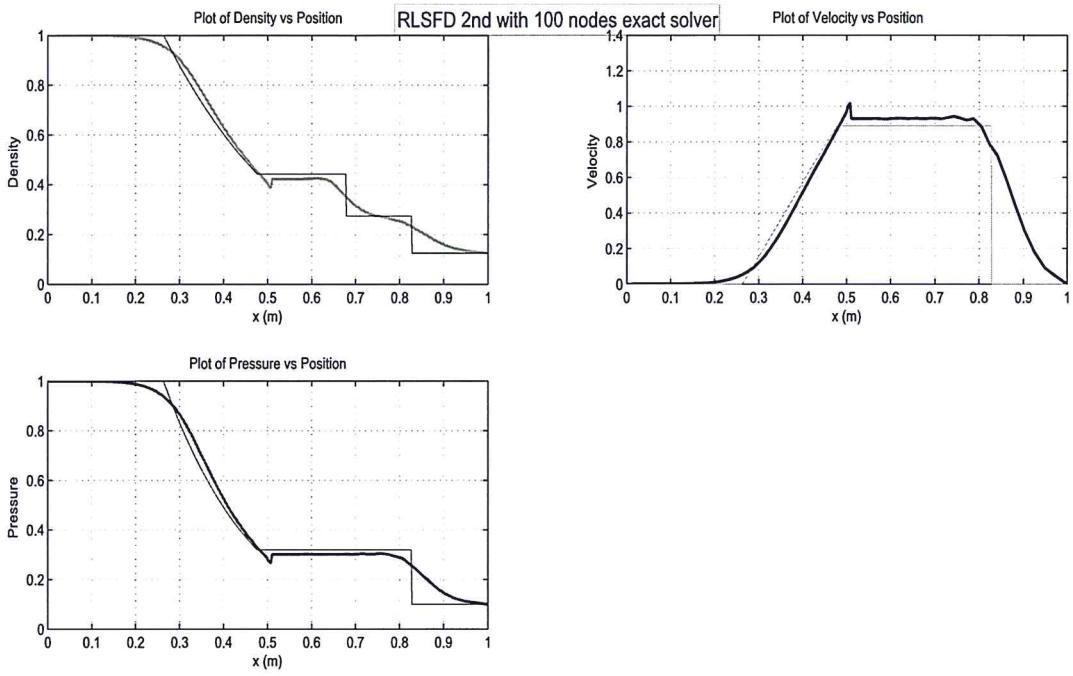

Figure 11: The *2nd* RLSFD scheme (Exact) with 100 nodes at $t = 0.2$

The figure below shows the exact Riemann solver for 50 nodes using the 2^{nd} RLSFD scheme.

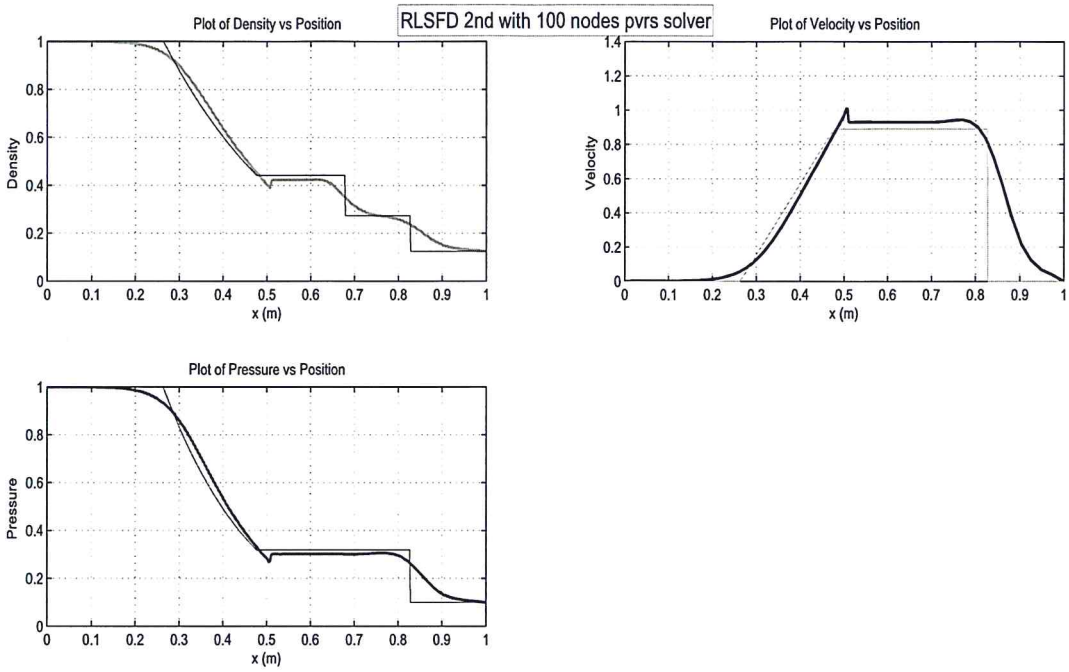

Figure 12: The $2nd$ RLSFD scheme (PVRS) with 100 nodes at $t = 0.2$

The 2^{nd} RLSFD scheme is more efficient when applied to a uniform grid with 100 nodes as shown in Fig.(13)

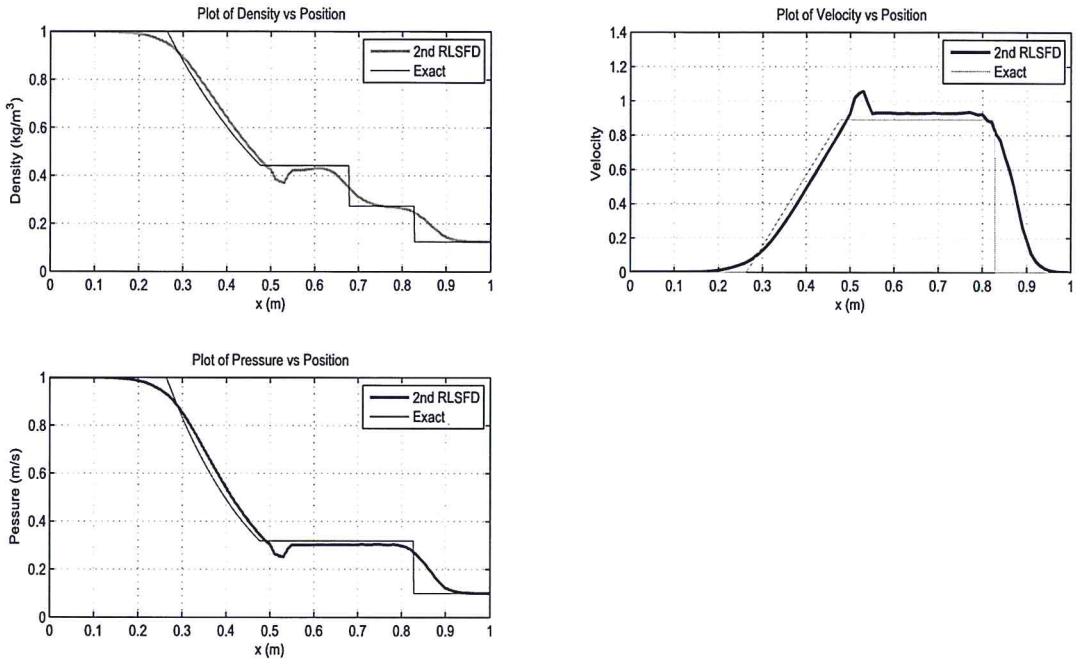

Figure 13: The *2nd* RLSFD scheme with uniform grid at $t = 0.2$

6.3 Extension to 2 dimension

We consider a two-dimensional Riemann problem for an ideal gas . The Euler equation for an ideal gas in 2D is :

$$U_t + F(U)_x + G(U)_y = 0, \tag{83}$$

where

$$U = \begin{pmatrix} \rho \\ \rho u \\ \rho v \\ \rho E \end{pmatrix}, F = \begin{pmatrix} \rho u \\ \rho u^2 + p \\ \rho uv \\ u(\rho E + p) \end{pmatrix}, G = \begin{pmatrix} \rho v \\ \rho uv \\ \rho v^2 + p \\ v(\rho E + p) \end{pmatrix}. \tag{84}$$

Here ρ is the density , u the velocity in the x-direction, v the velocity in the y-direction, E is the total energy and p is the pressure.

The initial data consists of a single constant state in each of four quadrants of the $x - y$ plane. The problem is solved in the $x - y$ region $(0, 1) \times (0, 1)$ and the four quadrants are given by dividing this region by two-lines $x = \frac{1}{2}, y = \frac{1}{2}$. We solve the Riemann problem for Eq. (84) with initial data

$$(\rho, u, v, p)(x, y, 0) = \begin{cases} (\rho_1, u_1, v_1, p_1) & \text{if } x > 0.5 \text{ and } y > 0.5, \\ (\rho_2, u_2, v_2, p_2) & \text{if } x < 0.5 \text{ and } y > 0.5, \\ (\rho_3, u_3, v_3, p_3) & \text{if } x < 0.5 \text{ and } y < 0.5, \\ (\rho_4, u_4, v_4, p_4) & \text{if } x > 0.5 \text{ and } y < 0.5, \end{cases} \tag{85}$$

The different admissible configuration for the polytropic gas consist of the forward rarefaction $\overrightarrow{R}$,backward rarefaction $\overleftarrow{R}$, forward shock $\overrightarrow{S}$, backward shock $\overleftarrow{S}$ and contact-wave $J^{\pm}$. (Kurganov & Tadmor (2002))

7 Numerical Experiment of the RLSFD scheme

First configuration consists of 4 backward shocks. The initial data is given by

$$\begin{aligned}(\rho_1, u_1, v_1, p_1) &= (1.5, 0, 0, 1.5)\\ (\rho_2, u_2, v_2, p_2) &= (0.5323, 1.206, 0, 0.3)\\ (\rho_3, u_3, v_3, p_3) &= (0.138, 1.206, 1.206, 0.029)\\ (\rho_4, u_4, v_4, p_4) &= (0.5323, 0, 1.206, 0.3)\end{aligned} \tag{86}$$

This is at $t = 0.3$ and Fig. (14) shows the solution in the region where these 4 shocks interact.

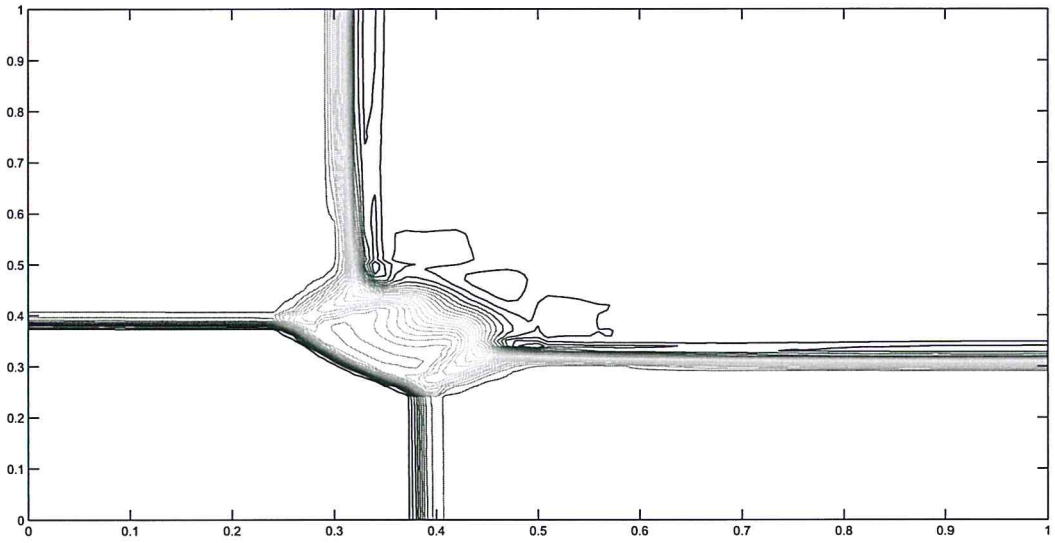

Figure 14: RLSFD scheme with 70 nodes with 32 contours

We observed that the RLSFD scheme located the shock interaction in the inner jump segments in the lower left quadrant .

The second configuration is a 2 backward shock and 2 forward shock. The initial data

are given by

$$\begin{aligned}(\rho_1, u_1, v_1, p_1) &= (1.1, 0, 0, 1.1)\\ (\rho_2, u_2, v_2, p_2) &= (0.5065, 0.8939, 0, 0.35)\\ (\rho_3, u_3, v_3, p_3) &= (1.1, 0.8939, 0.8939, 1.1)\\ (\rho_4, u_4, v_4, p_4) &= (0.5065, 0, 0.8939, 0.35)\end{aligned} \tag{87}$$

This is computed at $t = 0.25$

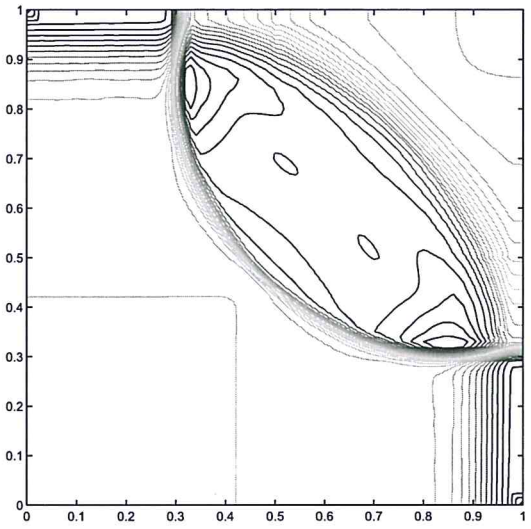

Figure 15: RLSFD scheme with 100 nodes with 32 contours

We observed that it resolve the shock well. But the solution is not symmetric in the lens axis, therefore has different upper and lower curved shocks.

The third configuration is 4 forward rarefaction (Toro & Toro (1999))

$$\begin{aligned}(\rho_1, u_1, v_1, p_1) &= (1, 0, 0, 1)\\ (\rho_2, u_2, v_2, p_2) &= (0.5197, -0.7259, 0, 0.4)\\ (\rho_3, u_3, v_3, p_3) &= (0.1072, -0.7259, -1.4045, 0.0439)\\ (\rho_4, u_4, v_4, p_4) &= (0.2579, 0, -1.4045, 0.15)\end{aligned} \tag{88}$$

This is at $t = 0.2$

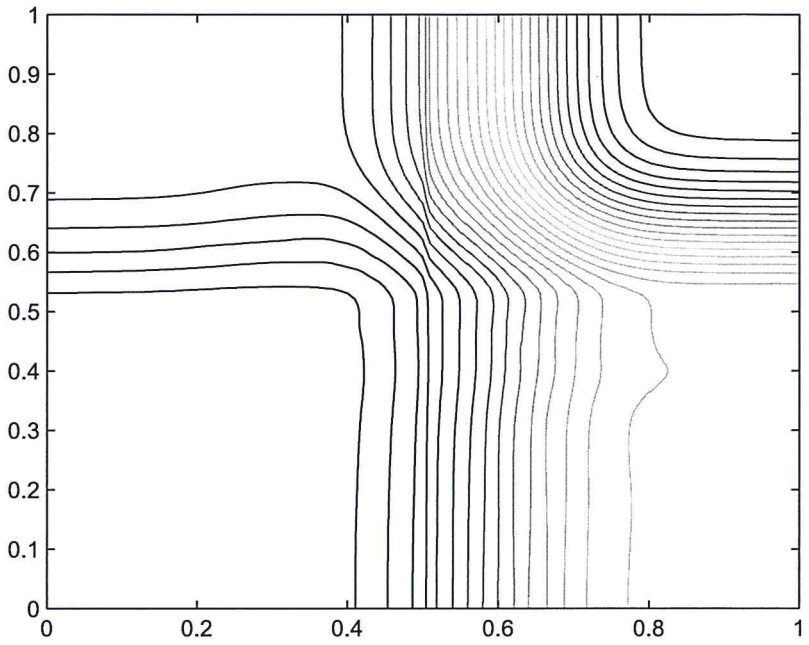

Figure 16: RLSFD scheme with 70 nodes with 32 contours

We observe in Fig.(16) that the RLSFD has the ability to resolve the 4 rarefaction waves in this configuration.

We consider another configuration which consist of 2 backward rarefaction and 2 forward rarefaction waves given by

$$\begin{aligned} (\rho_1, u_1, v_1, p_1) &= (1, 0, 0, 1) \\ (\rho_2, u_2, v_2, p_2) &= (0.5197, -0.7259, 0, 0.4) \\ (\rho_3, u_3, v_3, p_3) &= (1, -0.7259, -0.7259, 1) \\ (\rho_4, u_4, v_4, p_4) &= (0.5197, 0, -0.7259, 0.4) \end{aligned} \tag{89}$$

We observe in Fig.(17) that the scheme is dissipative in the lower left quadrant but was able to resolve the 4 rarefaction waves.

This is at $t = 0.2$

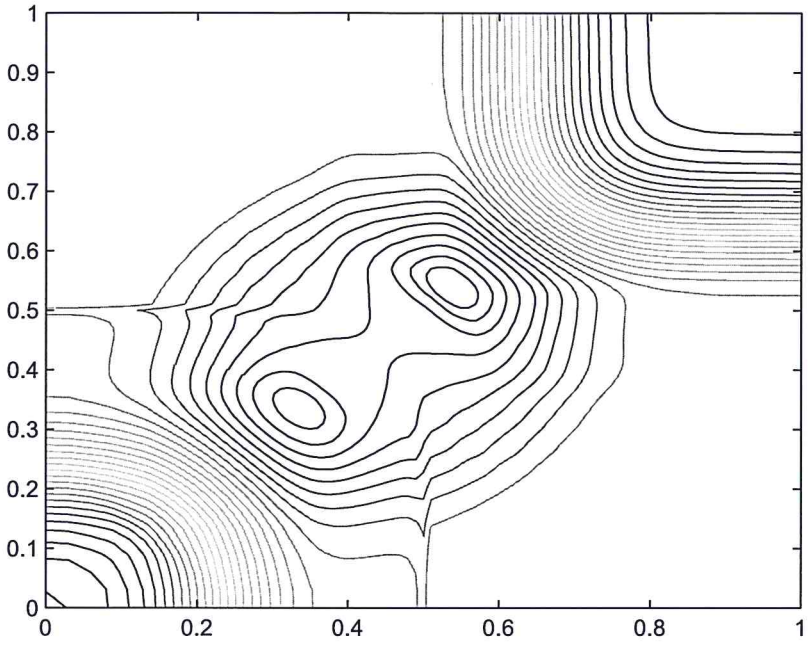

Figure 17: RLSFD scheme with 70 nodes with 32 contours

This configuration consist of 4 negative contact waves and the initial data is given by

$$\begin{aligned}(\rho_1, u_1, v_1, p_1) &= (1, -0.75, -0.5, 1)\\ (\rho_2, u_2, v_2, p_2) &= (2, -0.75, 0.5, 1)\\ (\rho_3, u_3, v_3, p_3) &= (1, 0.75, 0.5, 1)\\ (\rho_4, u_4, v_4, p_4) &= (3, 0.75, -0.5, 1)\end{aligned} \tag{90}$$

This is at $t = 0.23$

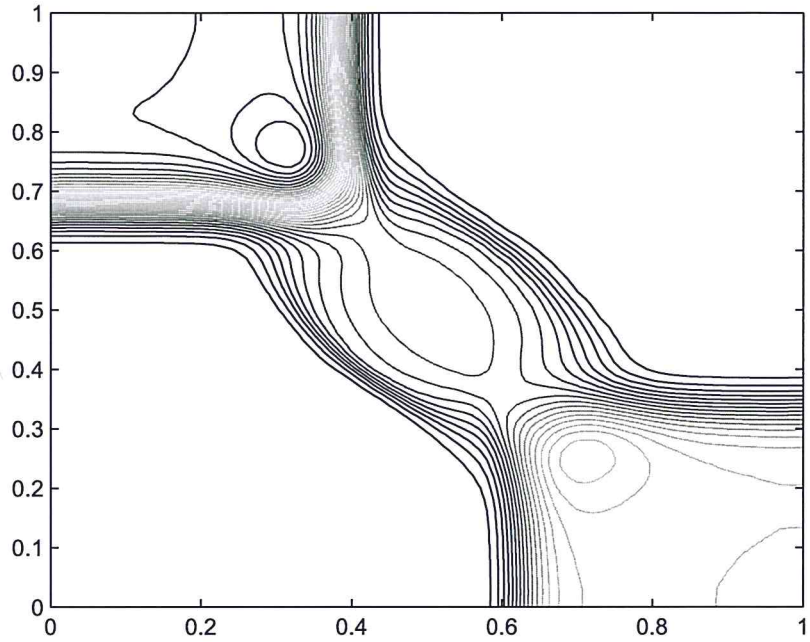

Figure 18: RLSFD scheme with 70 nodes with 32 contours

We consider a configuration of 2 negative contacts and 2 forward rarefaction and the initial data is given by:

$$\begin{aligned}(\rho_1, u_1, v_1, p_1) &= (1, 0.1, 0.1, 1)\\ (\rho_2, u_2, v_2, p_2) &= (0.5197, -0.6259, 0.1, 0.4)\\ (\rho_3, u_3, v_3, p_3) &= (0.8, 0.1, 0.1, 0.4)\\ (\rho_4, u_4, v_4, p_4) &= (0.5197, 0.1, -0.6259, 0.4)\end{aligned} \tag{91}$$

We observed in Fig.(19) that the RLSFD scheme has a good resolution on the stationary contact bordering the lower left quadrant. The RLSFD scheme preserve the symmetry quite well on this configuration about $(0,0),(1,1)$ diagonal. The scheme is dissipative on the upper right quadrant on the 2 forward rarefaction.

This is at $t = 0.25$

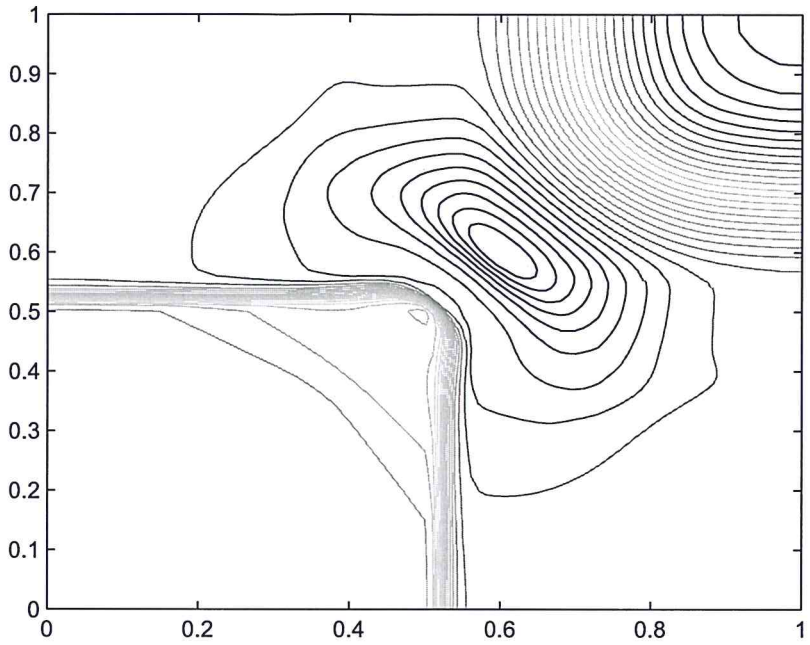

Figure 19: RLSFD scheme with 70 nodes with 32 contours

We consider a configuration of 2 negative contacts and 2 backward rarefaction and the initial data is given by:

$$\begin{aligned} (\rho_1, u_1, v_1, p_1) &= (0.5197, 0.1, 0.1, 0.4) \\ (\rho_2, u_2, v_2, p_2) &= (1, -0.6259, 0.1, 1) \\ (\rho_3, u_3, v_3, p_3) &= (0.8, 0.1, 0.1, 1) \\ (\rho_4, u_4, v_4, p_4) &= (1, 0.1, -0.6259, 1) \end{aligned} \tag{92}$$

This is at $t = 0.25$

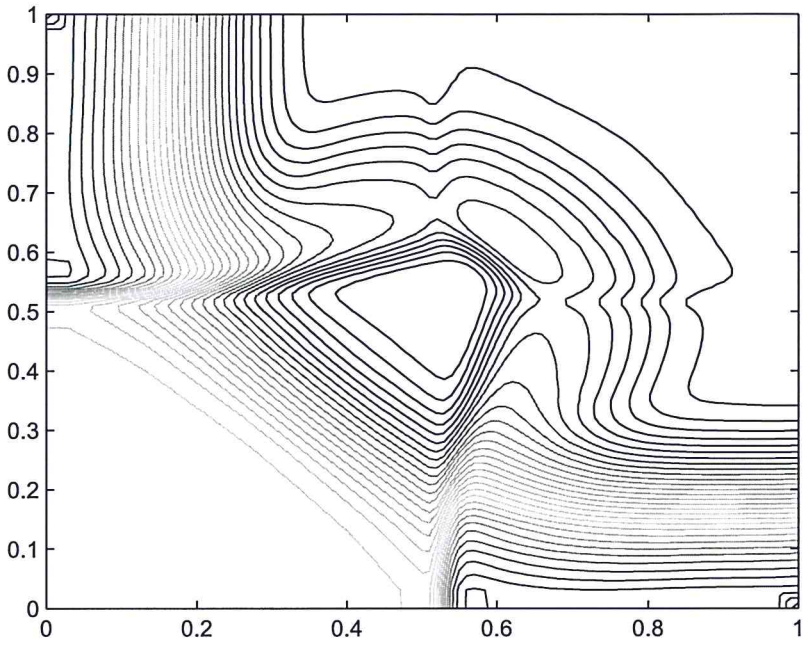

Figure 20: RLSFD scheme with 70 nodes with 32 contours

We have applied the RLSFD in 2-D for a two-phase flow. These test cases can be obtain from Rudman (1997). 2-d numerical experiment are conducted to validate our algorithm. First test case is a circle advected for $t = 0.2s$. Initially the circle with radius 0.2 and centered at $(0.5, 0.3)$. By solving the advection equation

$$\frac{\partial C}{\partial t} + \nabla.(UC) = 0. \tag{93}$$

The advection velocity U is $(1, 1)$.

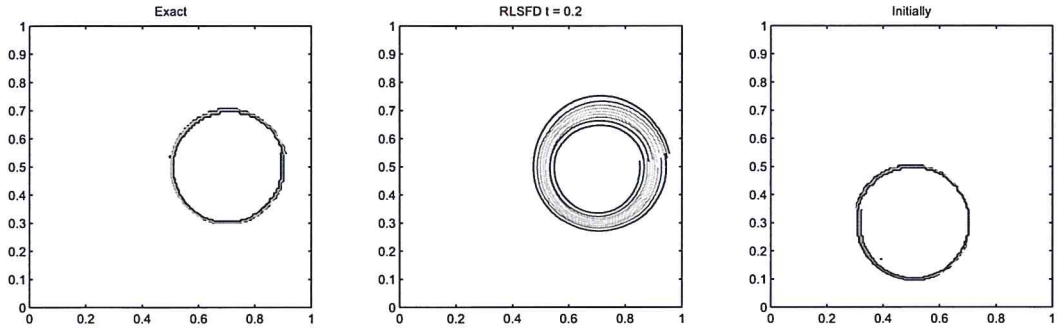

Figure 21: Circle using RLSFD at $t = 0.2$

The second test case is a squares advected for $t = 0.2$ with velocity $U = (1, 1)$. Initially the circle is center at $(0.5, 0.3)$.

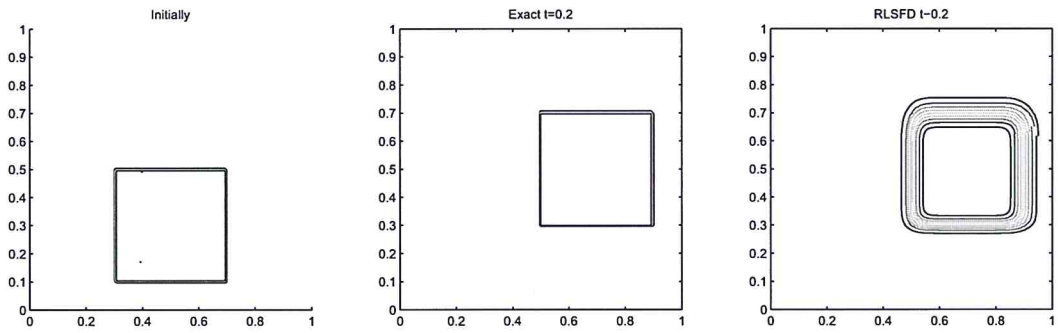

Figure 22: Square using RLSFD at $t = 0.2$

The compuatation are carried out on a 201 X 201 nodes . For the third test case, we advect a π-shape, for $t = 0.2s$ as shown in Fig.(23) . The computation are carried out on

a 201 X 201 computational mesh. The Pi-shape is centered at $(0.5, 0.3)$ and advected at a velocity $U = (1, 1)$.

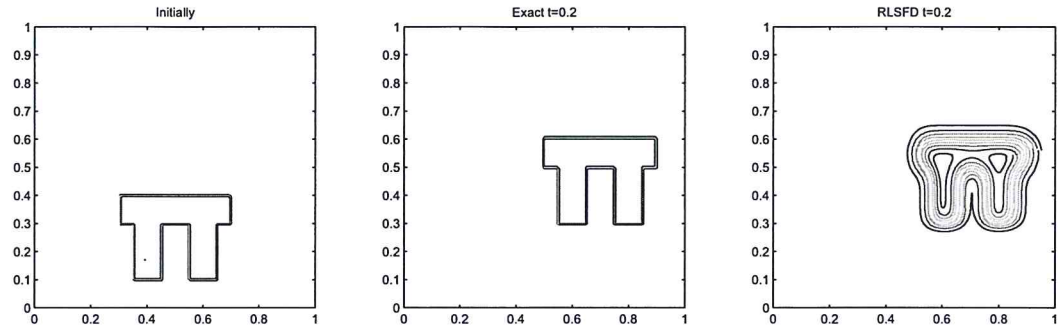

Figure 23: Pi shape using RLSFD at $t = 0.2$

The last test case is a slotted disk. This study is useful to test the accuracy of the reconstruction method and in particular its ability to represent fluid interfaces with high curvature. A circle with radius equal to 0.2 cells is centred in (0.5, 0.3) with a vertical rectangular cut is produced with width equal to $\frac{1}{3}$ of the radius and length $\frac{5}{3}$ of the radius of the circle. The velocity field $U = (u, v)$ can be expressed in terms of the stream function

$$\Psi(x, y) = -\frac{\Omega}{2}((y - y_0)^2 + (x - x_0)^2), \tag{94}$$

where $u = \frac{\partial \Psi}{\partial y}$ and $v = -\frac{\partial \Psi}{\partial x}$. Fig.(24) advected for $t = 0.2s$.

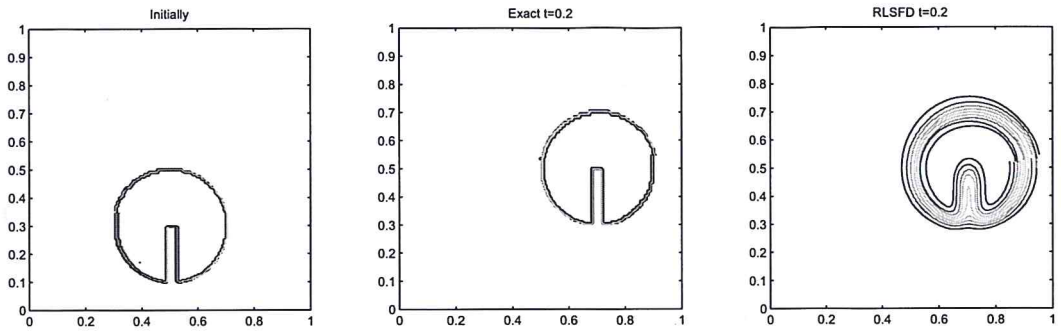

Figure 24: Slotted Disk using RLSFD at $t = 0.2$

8 Conclusion

We have described a new Riemann solver that is incorporated in the Least Square Finite Difference Scheme. We presented 3 types of schemes, namely, the first order Riemann Least Squares Finite Difference Scheme (RLSFD), the conservative form of the RLSFD scheme and the second order Riemann Least Squares finite difference scheme. We proved that the first order RLSFD is consistent with the linear advection equation and we also conducted its stability analysis. We proved the existence of a weak solution for the first order RLSFD. Finally, we presented our numerical results when the RLSFD was applied to the 1-D linear advection equation, 1-D Burgers equation, the Shock tube problem, the 2-D Riemann problem and to some two phase flow problems. Our numerical results show that the second order RLSFD captures discontinuity in inviscid flow quite accurately. One possible application of the scheme is in the simulation of traffic flows on highways.

9 Acknowledgement

The financial support of the project was kindly provided by the Mauritius Research Council (MRC) through the MRC unsolicited Research Grant scheme (MRC/RUN/1405) on the project K0378.

References

Harten, A., Lax, P. D. & Leer, B. v. (1983), 'On upstream differencing and godunov-type schemes for hyperbolic conservation laws', *SIAM review* **25**(1), 35–61.

Kurganov, A. & Tadmor, E. (2002), 'Solution of two-dimensional riemann problems for gas dynamics without riemann problem solvers', *Numerical Methods for Partial Differential Equations* **18**(5), 584–608.

LeVeque, R. J. (2002), *Finite volume methods for hyperbolic problems*, Vol. 31, Cambridge university press.

Osher, S. & Solomon, F. (1982), 'Upwind difference schemes for hyperbolic systems of conservation laws', *Mathematics of computation* **38**(158), 339–374.

Roe, P. L. (1981), 'Approximate riemann solvers, parameter vectors, and difference schemes', *Journal of computational physics* **43**(2), 357–372.

Rudman, M. (1997), 'Volume-tracking methods for interfacial flow calculations', *International journal for numerical methods in fluids* **24**(7), 671–691.

Toro, E. F. & Toro, E. F. (1999), *Riemann solvers and numerical methods for fluid dynamics*, Vol. 16, Springer.

Van Leer, B. (1979), 'Towards the ultimate conservative difference scheme. v. a second-order sequel to godunov's method', *Journal of computational Physics* **32**(1), 101–136.

Woodward, P. & Colella, P. (1984), 'The numerical simulation of two-dimensional fluid flow with strong shocks', *Journal of computational physics* **54**(1), 115–173.